Powder Technology 428 (2023) 118789

Contents lists available at ScienceDirect

Powder Technology

journal homepage: www.journals.elsevier.com/powder-technology

Square Cyclone Separator: Performance Analysis Optimization and Operating Condition Variations Using CFD-DPM and Taguchi Method

Hossein Fatahian [a], Esmaeel Fatahian [a], Rasool Erfani [b,c,*]

[a] School of Computing and Engineering, University of Huddersfield, HD1 3DH, UK
[b] Department of Engineering, Manchester Metropolitan University, Manchester M1 5GD, UK
[c] Department of Civil, Environmental and Geomatic Engineering, University College London, London WC1E 6BT, UK

HIGHLIGHTS

- Using 3D CFD to assess the square cyclone performance and consider operating parameters.
- Particle mass flow rate, inlet velocity, inlet temperature, and turbulent intensity were analyzed.
- Taguchi method was utilized to maximize separation efficiency.
- Separation efficiency achieved 76% with optimized values.

GRAPHICAL ABSTRACT

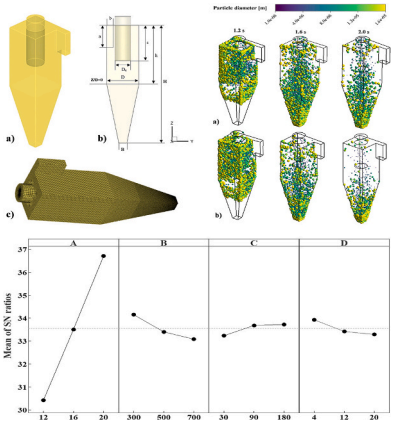

ARTICLE INFO

Keywords:
Square cyclone
CFD
Eulerian-Lagrangian
Optimization

ABSTRACT

The square cyclone separator is an efficient separation device for high-temperature gas within Circulating Fluidized Bed (CFB) boilers. Additionally, other operating factors such as particle loading and gas velocity are frequently thought to have considerable influence on fluid flow in gas cyclones, making parameter optimization essential. Finding the most suitable operating configuration can be challenging because of a fundamental understanding of the operating principles, which has yet to be taken into consideration in the literature. The gas flow inside a square cyclone was analyzed using Computational Fluid Dynamics (CFD) for investigating parameters including particle mass flow rate, inlet velocity, inlet temperature, and turbulent intensity in this research. The Taguchi method was utilized as a Design of Experiment (DoE) methodology to maximize separation efficiency. The Analysis of Variance (ANOVA) was conducted to evaluate the relative contribution of each parameter to the performance of the gas cyclone, while the Unsteady Reynolds-Averaged Navier-Stokes (URANS) equations were solved using the Eulerian-Lagrangian approach to represent particle movement. Also, Discrete Random Walk (DRW) was incorporated to account for velocity fluctuation. According to a Taguchi analysis, particle mass flow rate is the parameter that has the least impact on cyclone performance, whereas inlet velocity

* Corresponding author at: Department of Engineering, Manchester Metropolitan University, Manchester M1 5GD, UK.
E-mail address: r.erfani@mmu.ac.uk (R. Erfani).

https://doi.org/10.1016/j.powtec.2023.118789
Received 12 April 2023; Received in revised form 16 June 2023; Accepted 6 July 2023
Available online 11 July 2023

has the most contribution. From the different range of factors examined here, it is proved that the optimal levels of factors for inlet velocity, inlet temperature, particle mass flow rate, and turbulent intensity are, respectively, 20 m/s, 300 K, 180 g/min, and 4%.

Nomenclature

C_D	Drag coefficient
K	Fluctuating kinetic energy (m^2/s^2)
P_f	Fluctuating energy production (m^2/s^3)
ν	Kinematic viscosity (m^2/s)
d_p	Particle diameter (μm)
g	Gravitational acceleration (m/s^2)
P	Pressure (Pa)
μ	Dynamic viscosity (kg/ms)
Re_p	Reynolds number
R_{ij}	Reynolds stress tensor
t	Time (s)
V	Velocity (m/s)
u_p	Particle velocity (m/s)
u_i	Gas velocity (m/s)
ε	Turbulence dissipation rate (m^2/s^3)
ρ	Density (kg/m^3)
ρ_p	Particle density (kg/m^3)

1. Introduction

Cyclone separators are inertial dust collectors that remove particles from the air by utilizing centrifugal force. Due to simple construction, inexpensive production and maintenance cost, and flexibility to a broad variety of working environments, including sizes and low rates [1,2], a cyclone is the most extensively used particle removal equipment. Since the separation in gas cyclones is mostly determined by particle inertial force, the conventional separator indicates lower separation efficiency for tiny particles [3,4]. Filtering particles from an air stream is a common practice in many processes, notably chemical processes, oil refining, petrochemical products, pharmaceutical, agriculture, and mineral extraction, to preserve the environment and public health from harmful impacts [5]. Cyclones are frequently classified as square or conventional [6–8]. In the industry, a traditional cylinder-shaped gas cyclone has long been in use. Cyclones with square-shaped bodies rather than cylindrical ones were first developed in the past three decades. The industrial world is still not familiar with square cyclones very well. Even so, they have many advantages over conventional ones, including simpler manufacture, simple boiler integration, and higher thermal efficiency when employed in conjunction with CFB boilers [3]. In CFB boiler operations, a square cyclone is utilized for separating coal combustion products. Several works have reported on the employment of square cyclones in CFB technology [9,10]. Square cyclone is superior to traditional one in several ways, such as faster construction, better timings for start-and-stop, and simpler engagement with the boiler [11]. The cyclone performance, whether conventional or square, for separating an incoming particle in feed gas and the pressure drop are assessed to evaluate its effectiveness. Different variables can influence the efficiency of particle collection or drop in pressure in a cyclone, including the physical properties of the material approaching the gas cyclone, operational circumstances, geometry or design, and airflow within the gas cyclone. Many works have been done to assess the effectiveness of gas cyclone separators, specifically regarding their ability to collect particles efficiently [12–17]. Wasilewski et al. [9] evaluated vortex finder modifications and placement length of the square cyclone on its efficiency. They revealed that the size and vortex finder shapes have a remarkable influence on gas cyclones. Through the use of a laminarizer, Huang et al. [13] augmented the performance of the cyclone and obtained a superior cyclone showing a reduction of 50% in particle size. For improving the collecting efficiency of a standard cyclone, Karagoz et al. [14] recommended changing the conical section and implementing a vortex control method. They showed that the novel cyclone can deliver much improved collecting efficiency while having a nearly identical pressure drop to a traditional cyclone. Furthermore, various experimental studies on square cyclones have been conducted to study the airflow within gas cyclones in terms of configurations [9,10,15]. Hosseini [16] analyzed the input geometry of the internal flow of the gas cyclone. Unique intake types, namely straight, angled, and curve inlets, were particularly adopted for enhancing the particle separation in a cyclone. He demonstrated that although inlets with bends and an inclination raised pressure loss, the removal efficiency was enhanced.

In many industrial processes, including the production of chemical materials, separating exhaust gas from the chimney, and various operations in thermal power plants, it is crucial to separate particles from hot gas [18]. By using the proper materials and construction, gas cyclones are utilized in scenarios where there are high-pressure, high-temperature, or corrosive gases. Thermo-physical characteristics of the fluid vary with temperatures. The working fluid temperature affects the gas cyclone performance consequently [18]. In accordance with the literature, only a few research have been carried out to investigate cyclone performance under harsh working circumstances [19,20]. The impact of input temperatures and velocities was examined by Gimbun et al. on pressure drop [21]. They observed that the pressure loss declines by rising inlet temperature. Siadaty et al. [22] conducted a thorough investigation to look at how flow and particle temperatures affect cyclone effectiveness. According to their findings, increasing the input temperature caused the tangential velocity to become maximum at a particular section. Furthermore, particle mass loading influence on gas cyclone efficiency, particularly that of square cyclones, has been insufficiently studied. As the mass loading approaches a maximum of 500 g/m^3, both gas tangential velocity and pressure drop within the gas cyclone decline [23]. As a result of the sweeping movements of larger particles and the accumulation of smaller particles within a cyclone structure, the separation ratio increases with particle mass loadings [23,24]. A separation efficiency may be augmented when the particle mass loading rises [24–26]. Wan et al. [27] evaluated the solid concentration of various particle sizes numerically using the Lagrangian approach inside a gas cyclone. They demonstrated that when the solid loading grew, the swirl was reduced, and the involvement of solid particles significantly changed the field of gas flow.

The presented literature review demonstrated that operating conditions and gas flow characteristics were paid less attention by researchers than cyclone design and parametric analysis. Because the square gas cyclone is usually used in CFB boilers, the working fluid temperature is actually quite high. Additionally, the experimental and numerical data on how particle mass flow rate affects square cyclone performance are relatively limited. According to the literature survey, there has not been a systematic strategy for optimizing the operating conditions of square cyclone separators. The Taguchi approach is used in this work to propose a numerical model and design methodology for a square cyclone separator.

Additionally, an analysis of variance is performed using the data collected from the orthogonal arrays from the Taguchi analysis to offer credibility in the robust design methodology implemented. The ANOVA application allows for a more in-depth analysis of the influence of each

design parameter and its relative importance to the performance of square cyclones. This study represents the initial endeavor to statistically analyze and optimize the effect of various operational factors on the efficacy of square cyclones in removing particles.

2. Numerical modeling

2.1. 3D model

Figs. 1 (a) and (b) depict a conceptual aspect and 3D design of the cyclone in accordance with an experimental test done by Su and Mao [28]. The variables of the geometry of the gas cyclone are summarized in Table 1. ANSYS-ICEM CFD was used in the present research to generate a hexahedral grid, as shown in Fig. 1 (c).

2.2. Turbulence modeling

The turbulence model used is a crucial element that impacts the correctness of the complex flow field. The precision of CFD of the air inside the gas cyclone is based on an appropriate definition of the turbulent characteristics of the flows [29]. In the present study, a three-dimensional CFD analysis was implemented to assess the flow field within the cyclone. The following are the conservation equations of mass and momentum in the incompressible flow: [30]:

$$\frac{\partial \overline{u}_i}{\partial x_i} = 0 \tag{1}$$

$$\frac{\partial \overline{u}_i}{\partial t} + \overline{u}_j \frac{\partial \overline{u}_i}{\partial x_j} = -\frac{1}{\rho}\frac{\partial \overline{P}}{\partial x_i} + \nu \frac{\partial^2 \overline{u}_i}{\partial x_j \partial x_j} - \frac{\partial}{\partial x_j} R_{ij} \tag{2}$$

where $\overline{u}_i$ is the mean velocity, x_i represents the spatial position, ρ corresponds to density, and ν represents kinematic viscosity. Also, $\overline{P}$ corresponds to mean pressure and $R_{ij} = \overline{u_i' u_j'}$ represents the tensor of Reynolds stress, where $u_i' = u_i - \overline{u}_i$ denotes the ith fluctuating velocity component.

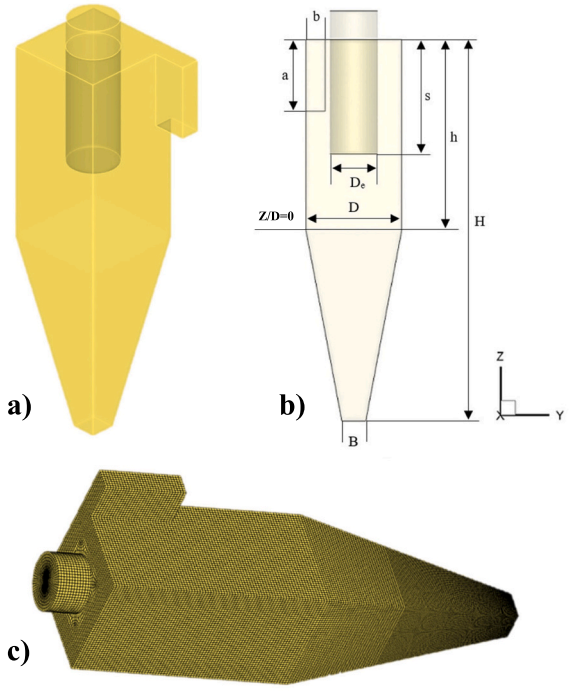

Fig. 1. An illustration of a) a three-dimensional model, b) geometric specification, and c) hexahedral mesh.

Table 1
Dimension (D = 200 mm).

Dimension	D_e/D	a/D	b/D	s/D	h/D	H/D	B/D
Gas cyclone	0.5	0.75	0.2	1.2	2	4	0.25

The standard k-ε, RNG k-ε, and realizable k-ε models are not suited for the non-axisymmetric, 3D, and highly swirling flow in cyclone separator [19]. However, studies have demonstrated that the Reynolds Stress Model (RSM) and Large Eddy Simulation (LES) adequately represent swirling flows within cyclones [9,31–34]. The LES method offers more accurate findings than the RSM for estimating the flow within cyclones, but it has higher computational costs. As a result, RSM was used for this work for modeling the complex rotating two-phase flow of the square cyclone. Seven partial differential equations [35,36] are included in the RSM model which can be defined as [37]:

$$\frac{\partial}{\partial t}R_{ij} + \overline{u}_k \frac{\partial}{\partial x_k}R_{ij} = \frac{\partial}{\partial x_k}\left(\frac{\nu_t}{\sigma^k}\frac{\partial}{\partial x_k}R_{ij}\right) - \left[R_{ik}\frac{\partial \overline{u}_j}{\partial x_k} + R_{jk}\frac{\partial \overline{u}_i}{\partial x_k}\right] - C_1\frac{\varepsilon}{K}\left[R_{ij} - \frac{2}{3}\delta_{ij}K\right] - C_2\left[P_{ij} - \frac{2}{3}\delta_{ij}P\right] - \frac{2}{3}\delta_{ij}\varepsilon \tag{3}$$

where, P_{ij} can be written as [38]:

$$P_{ij} = -\left[R_{ik}\frac{\partial \overline{u}_j}{\partial x_k} + R_{jk}\frac{\partial \overline{u}_i}{\partial x_k}\right], P_f = \frac{1}{2}P_{ij} \tag{4}$$

with P_f denotes the fluctuating energy production, ν_t representing turbulent (eddy) viscosity, and $\sigma^k = 1$, $C_1 = 1.8$, $C_2 = 0.6$ show empirical constants. The transport equation of turbulence dissipation rate, ε, may be written as follows [39]:

$$\frac{\partial \varepsilon}{\partial t} + \overline{u}_j \frac{\partial \varepsilon}{\partial x_j} = \frac{\partial}{\partial x_j}\left(\left(\nu + \frac{\nu_t}{\sigma^\varepsilon}\right)\frac{\partial \varepsilon}{\partial x_j}\right) - C^{\varepsilon 1}\frac{\varepsilon}{K}R_{ij}\frac{\partial \overline{u}_i}{\partial x_j} - C^{\varepsilon 2}\frac{\varepsilon^2}{K} \tag{5}$$

$K = \frac{1}{2}\overline{u_i' u_i'}$ represents the fluctuating kinetic energy, and ε corresponds to the turbulence dissipation rate. The constants values are $\sigma^\varepsilon = 1.3$, $C^{\varepsilon 1} = 1.44$, $C^{\varepsilon 2} = 1.92$.

2.3. Discrete phase model (DPM) eqs

A model was developed for the two-phase flow using an Eulerian-Lagrangian methodology in Ansys Fluent CFD solver. To address the gas phase as continuous, this technique involves computing momentum equations while tracking particles across the fluid domain and was used to study the solid phase (discrete phase) [40]. Particle-particle interactions could be neglected if the volume fraction of the dispersed second phase is small [26]. In the present work, the average particle volume fraction is 7.7×10^{-6}. The two-way coupling technique, which effectively addresses particle interaction with gas flow, was employed since particle contact was negligible, and throughout most areas, the volume fraction of particles should be $<10^{-3}$ [26]. Through the specification of particle size and density, the DPM was implemented to assess particle trajectories in a Lagrangian reference frame [15,46]. Due to fluid phase turbulence, the stochastic tracking model predicts particle dispersion. Using stochastic approaches, this model accurately depicts how fluctuations of instantaneous turbulent velocity affect particle trajectories [22]. In order to investigate turbulent particle dispersion, a DRW model [41] was used in the proposed numerical simulations. The distribution of particle size was evaluated through a Rosin-Rammler equation. Morsi and Alexander's [42] equation and the relative Reynolds number (Re_p) can be used to account for the drag coefficient of spherical particles. The particle motion equation is as follows [43]:

Table 2
Solver setting.

Turbulence model	Unsteady	RSM
Solution methods	Pressure-velocity coupling	SIMPLEC
Spatial discretization	Pressure	PRESTO!
	Momentum	Quick
	Turbulent kinetic energy	Second-order upwind
	Specific dissipation rate	Second-order upwind
	Reynolds stress	First-order upwind
Convergence criteria	All equations	10^{-5}

$$\frac{d\vec{x}_p}{dt} = \vec{u}_p \tag{6}$$

$$\frac{d\vec{u}_p}{dt} = F_D\left(\vec{u} - \vec{u}_p\right) + \vec{a} \tag{7}$$

In Eq. (7), the first term on the right-hand side is the drag force in which:

$$F_D = \frac{18\mu}{\rho_p d_p^2}\frac{C_D Re_p}{24} \tag{8}$$

where ρ_p and d_p are the particle density and diameter, respectively, C_D represents the drag coefficient, u_i and u_p are the instantaneous gas and particle velocity, respectively.

The second term in Eq. (7) is the acceleration of gravity including buoyancy given as:

$$\vec{a} = \vec{g}\left(\frac{\rho_p - \rho}{\rho_p}\right) \tag{9}$$

$$Re_p = \frac{\rho_p d_p\left|\vec{u} - \vec{u}_p\right|}{\mu} \tag{10}$$

In Eq. (10), g_i corresponds to gravitational acceleration and Re_p is the relative Reynolds number. μ is related to the dynamic viscosity.

2.4. Boundary condition

The gas flow equations were investigated by implementing a finite volume approach. In the present CFD analysis, the steady solver (gas alone) was employed for the first 10,000 iterations before switching to the unsteady solver (particle tracking) by 10^{-4} s for time-step and a particle feeding flow time of 0.5 to 1.0 s. For efficiency computations, the simulation flow time was 3.5 s in total. The gas volumetric flow rate and gas cyclone volume both had an impact on residence time [44]. Applying an RSM turbulence model and a standard wall function according to the intense swirling flow in a cyclone separator, the effect of turbulence was examined [15,45]. A condition with 10,000 Fly ash particles and a density of 1989.7 kg/m^3 was developed. A coal-fired boiler on the inlet surface of a power plant with size distributions (1 to 32 μm) was used to inject into the square cyclone. The parameters of the CFD solver adopted in the current investigation are demonstrated in Table 2. For the boundary condition, the gas inflow velocity was constant at the inlet, and it was additionally thought that particle and intake velocities were the same. The inlet velocity range was set at 12 to 28 m/s and hydraulic diameter and turbulence intensity were both adjusted to 0.0857 m and 4%, respectively [46,47]. The gas exit was considered to be the outflow. A dust outflow region was modified to fulfill the DPM condition, and the walls of the square cyclone were set to no-slip condition.

Table 3
Thermo-physical values [20,22,48,49].

T (K)	ρ (kg/m^3)	μ × 10^5 (Pa.s)
300	1.192	1.827
500	0.6964	2.701
700	0.4975	3.388

Table 3 provides information on the density and viscosity of a gas phase (air) at different temperatures. The temperature ranges that were mentioned in prior research served as the basis for the selection of the temperature values [20,22,48,49]. It was assumed that the gas flow was isothermal but at diverse temperature values in the current study since heat transfer was not addressed. But on the other side, the cyclone separator performance was examined concerning the impact of temperature dependency on gas thermo-physical parameters. To assess particle mass loading on square cyclone efficiency, and fluid flow at different temperatures, the minimum ($T = 300$ K), medium ($T = 500$ K), and highest ($T = 700$ K) temperatures were selected for the current study. Additionally, three particle mass flow rates of 30, 90, and 180 g/min were chosen in terms of inlet velocities (12 m/s, 16, and 20 m/s). These values are selected to be consistent with the available experimental data.

2.5. Verification of mesh independence

A grid size has a significant impact on the convergence and precision of the simulated outcomes in CFD. In this study, the grid independence of the square cyclone was verified. Different grid sizes were applied to attain this purpose. Three different mesh levels (coarse, medium, and fine) were generated including 480,000, 720,000, and 1,080,000 elements, respectively. The profiles of pressure for mentioned meshes at Z/D = 0.75 are illustrated in Fig. 2. As a result of the pressure difference being <1% between two successive meshes, the computational results demonstrated mesh independence. As a basis, a medium mesh (720,000 cells) was used for subsequent CFD modeling. This mesh maintained a suitable level of grid independence while achieving shorter processing costs.

2.6. Validation of numerical simulation

Su and Mao's [28] experimental data and Su et al. [50] numerical outcomes for a square cyclone were considered to confirm the computational model and verify the CFD simulation, see Figs. 3 and 4. The CFD conditions were adopted to be equivalent to those implemented in other works [28,50]. Between the experimental data and the estimated pressure drop, there was a minimum 8% discrepancy. The experiments and current simulations are in agreement with one another, proving that the

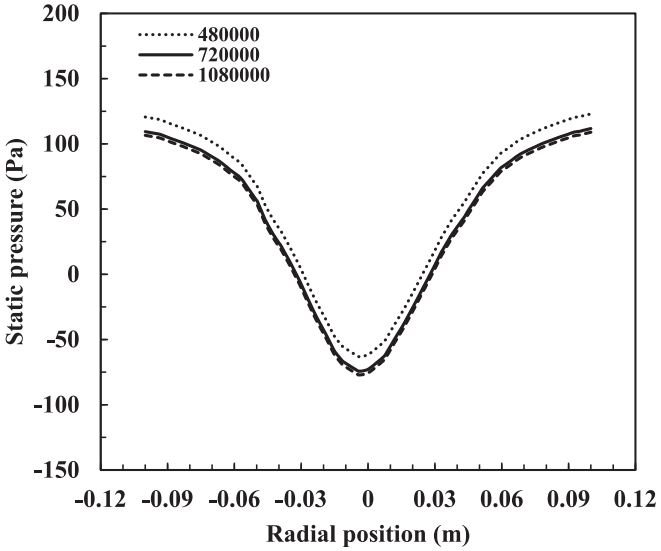

Fig. 2. Profiles of radial static pressure at 12 m/s.

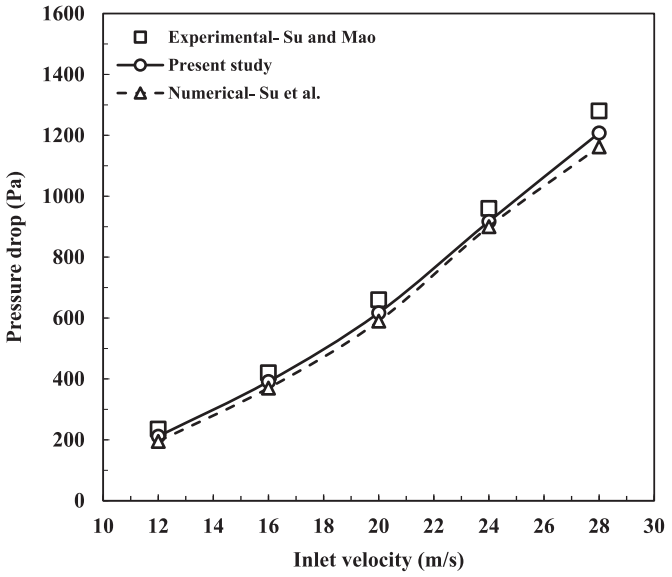

Fig. 3. Comparing pressure drop with Su and Mao [28] experimental test and Su et al. [50] CFD findings.

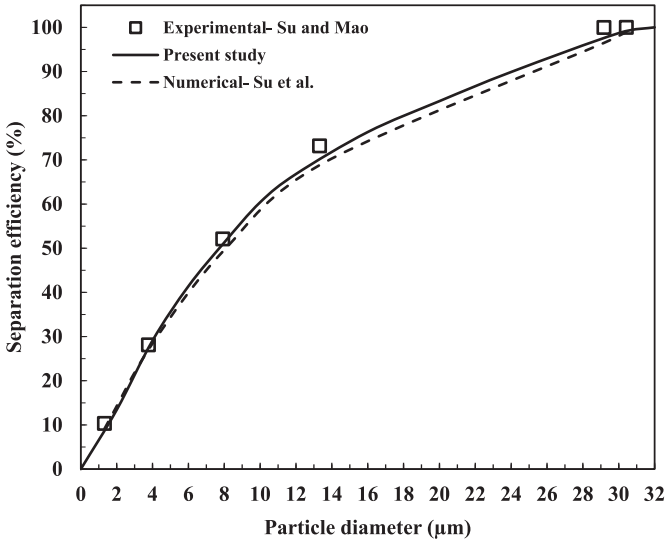

Fig. 4. Comparing the separation efficiency at V = 20 m/s with Su and Mao [28] experimental data and Su et al. [50] numerical results.

current technique can accurately anticipate the performance of a square cyclone considering the efficiency and pressure drop.

3. Results and discussion

3.1. Optimization procedure

Response Surface Methodology (RSM) and the Taguchi method are two common methods that generate the Design of Experiment (DoE) according to the measured parameters of the response variable and

Table 4
Relevant data about the variables and levels that correspond to the control parameters.

Factors	Control parameters	Notations	Level 1	Level 2	Level 3
A	Inlet velocity	V	12	16	20
B	Inlet temperature	T	300	500	700
C	Particle mass flow rate	R	30	90	180
D	Turbulent intensity	TI	4	12	20

experiment details to be modified [51,52]. Finding the optimal design of systems [53,54] with the minimum number of experiments is made possible by the Taguchi approach, which is both efficient and cost-effective. In the context of a gas cyclone separator, the Taguchi approach can be used to enhance the efficiency and effectiveness of the separator's performance. The aim of applying the Taguchi technique in this context is to identify the control factors that considerably influence the gas cyclone performance and determine the optimal levels of these factors to achieve the desired outcome.

Seven stages build up the process of determining the optimal parameters. Fig. 5 indicates the block diagram of the optimization procedure. Here, the operating conditions for a square cyclone separator were optimized using the Taguchi technique. The primary steps of the Taguchi methodology comprise identifying the objective variables, choosing design parameters, creating orthogonal arrays for design variables, conducting experiments according to the orthogonal arrays, and examination of the experiments.

3.2. Objective functions

The loss function of Taguchi was defined to measure how much the system performance is affected by the deviation of an objective variable from its target value. The loss function could be adapted according to the specific objective value, and in this study, the goal was to maximize the separation efficiency. This resulted in the definition of the loss function as:

$$L(y) = \frac{K}{y^2} \tag{11}$$

where L denotes the loss function, K corresponds to a constant, and y represents the measured value that is related to the separation efficiency of this work.

3.3. Factor and level

The parameter design experiments established an optimized set of parameter responses to be one that results in a low-cost design with an adequate quality variation. The factor levels with the highest S/N ratio should be selected to determine the optimum quantity of each factor. The optimum combination of controlling parameters needs to be determined using the Taguchi approach. In this study, four critical factors, inlet velocity (V), inlet temperature (T), particle mass flow rate (R), and turbulent intensity (TI) have considerable influences on cyclone performance which are selected. The experiments are arranged following the orthogonal arrays of the parameters of the design after the determination of the design parameters and levels for each variable. Nine designed numerical experiments were provided by the L_9 orthogonal array of Taguchi, which was utilized in this case. Table 4 shows

Fig. 5. Block diagram of the whole optimization process.

Table 5
L_9 (3^3) orthogonal array.

Experiment	Factor/Level			
	Inlet velocity (A)	Inlet temperature (B)	Particle mass flow rate (C)	Turbulent intensity (D)
1	1	1	1	1
2	1	2	2	2
3	1	3	3	3
4	2	1	2	3
5	2	2	3	1
6	2	3	1	2
7	3	1	3	2
8	3	2	1	3
9	3	3	2	1

details on the factors and their levels concerning the control parameters.

3.4. Orthogonal array

The L_9 orthogonal array was used in computational experiments to evaluate the ideal design parameters that enhance separation efficiency. The numerical experiment results were utilized to establish the best design parameters. Signal-to-noise (S/N) ratio was adopted to characterize how the design parameters affected separation efficiency. The S/N ratio measures how noise effects influence system response. According to the expected system responses, three sorts of S/N ratios can be defined: larger-the-better (LB), nominal-the-better (NB), and smaller-the-better (SB). The square cyclone separator would perform better in this study with a greater particle separation efficiency. Therefore, the best design parameters were chosen using the larger-is-better S/N ratio. The larger-the-better S/N ratio is [47]:

$$S/N = -10log\left(\sum_{i=1}^{n}\frac{1}{n}\frac{1}{y_i^2}\right) \quad (12)$$

where n denotes the number of numerical experiments and y_i represents the separation efficiency. Instead of testing all possible scenarios, the Taguchi technique only requires a set number of experiments to examine according to the orthogonal array (OA). The standard OA L_9 (3^3) is used in this research as only four factors and three levels were considered, as listed in Table 5.

3.5. S/N ratio analysis

Table 6 presents the separation efficiency values and S/N ratios for each numerical experiment according to the orthogonal array. Here, the optimization is done on a particle diameter of 16 μm. The findings in Table 5 demonstrate that higher separation efficiency can be obtained by a larger S/N ratio. In addition, cyclone performance was considerably affected by inlet velocity. It can also be seen that E7 has the highest and E3 has the lowest separation efficiency. Higher values of inlet temperature deteriorate the collection of particles by the system. Enhanced inlet temperature caused a substantial reduction in centrifugal force, which decreased separation efficiency [49]. While the inlet temperature equal to 300 K enhanced the efficiency of a square cyclone. Additionally, higher inlet velocity was observed to improve the efficiency, as it raised the tangential velocity dramatically [49].

For each of the levels in each variable, the mean S/N ratio may be determined using the findings in Table 5. Fig. 6 depicts the profiles of the mean S/N ratio for four components at various values. From the value changes demonstrated in this figure, it is possible to identify the order of effectiveness of the chosen factors. This means that, among the four parameters examined in this study, factor A (inlet velocity) would have the most impact on the operation of a square cyclone was performed. When comparing the influences of inlet temperature and particle mass flow rate, the latter would have a minor effect. According to the result presented in Fig. 6, the combination of A_3, B_1, C_3, and D_1 estimates the highest separation efficiency using the mean S/N ratio values from a Taguchi approach. The contribution ratio of each parameter is presented in Fig. 7. Interestingly, the inlet velocity has 74.1% of the total effect. It demonstrates that factor A, which is inlet velocity, is the most notable factor among the four tested factors that influences cyclone performance. Furthermore, factor C (particle mass flow rate) has the least impact on efficiency.

3.6. ANOVA

ANOVA was carried out in this study to quantify the desirable and undesirable factors according to F-value and *P*-value. The regression analysis for separation efficiency against inlet velocity, inlet temperature, particle mass flow rate, and turbulent intensity has been conducted. Tables 7 and 8 present the ANOVA and regression analysis findings. The source of variation, degree of freedom (DF), the sum of squares (SS), mean square (MS), F and *P* values are presented in Table 8. The following findings are the result of this analysis. The *P*-value for inlet velocity is lower ($P < 0.05$). This suggests that this factor has a remarkable effect on the separation. Furthermore, the *P*-values for inlet temperature, particle mass flow rate, and turbulent intensity are large ($P > 0.05$). It highlights that these factors have a weak impact on separation efficiency. The regression analysis was done at a 95% confidence level significance level of $\alpha = 0.05$). ANOVA outcomes revealed that the P-value for regression is 0.001 and the F-value is 54.37S. The P-value is <5%, indicating that the produced model is correctly specified. Furthermore, this model estimated R^2 value is 96.4% and it underlines the reliability of the model.

3.7. Particle separation efficiency

Fig. 8 presents the variations in particle separation efficiency of the square cyclone as a function of particle diameter for the worst and optimized cases, E3 and E7, respectively. According to the collected particles in the bottom section, the DPM model was used to estimate the separation efficiency. With the increase in particle size, the separation efficiency was improved in both cases. Due to a greater inlet velocity than the E3 case, the optimized case (E7) exhibits higher separation efficiencies for all particle sizes. This is because when inlet velocity increases, a larger tangential velocity is generated [49]. Additionally, the collection of particles is negatively impacted by higher inlet temperature levels. Even though both cases have an equivalent particle mass loading, the square cyclone is more efficient to capture small particles at a low inlet temperature (300*K*).

3.8. Mean tangential velocity

Fig. 9 demonstrates the distribution and contours of the tangential velocity at Z/D = 0.75 (below the vortex finder) for the E3 and E7 cases. The tangential velocity distribution in both cases consists of a free vortex in the outer region and a forced vortex in the inner region (V-shaped), offering the predicted Rankine-type vortex [49]. Tangential velocity is almost evenly distributed along the center axis of the square cyclones. Furthermore, the region between the inner and outer vortices has the greatest tangential velocity [33].

A comparison of the results shown in Fig. 9 reveals that operating conditions have considerable effects on the distribution of the tangential velocity. Tangential velocity increases substantially in the free and forced vortex zones for the E7 optimized case. Since it has a higher inlet velocity and a lower inlet temperature. Previous research [19,22,49]

Table 6
Comparison of separation efficiency and S/N ratios.

Case	Inlet velocity (A)	Inlet temperature (B)	Particle mass flow rate (C)	Turbulent intensity (D)	Separation efficiency (%)	S/N ratio
E1	12	300	30	4	35.9	31.10
E2	12	500	90	12	32.7	30.29
E3	12	700	180	20	31.2	29.88
E4	16	300	90	20	50.1	33.40
E5	16	500	180	4	49.7	33.93
E6	16	700	30	12	42.7	32.61
E7	20	300	180	12	73.8	37.36
E8	20	500	30	20	63.1	36.00
E9	20	700	90	4	68.9	36.76

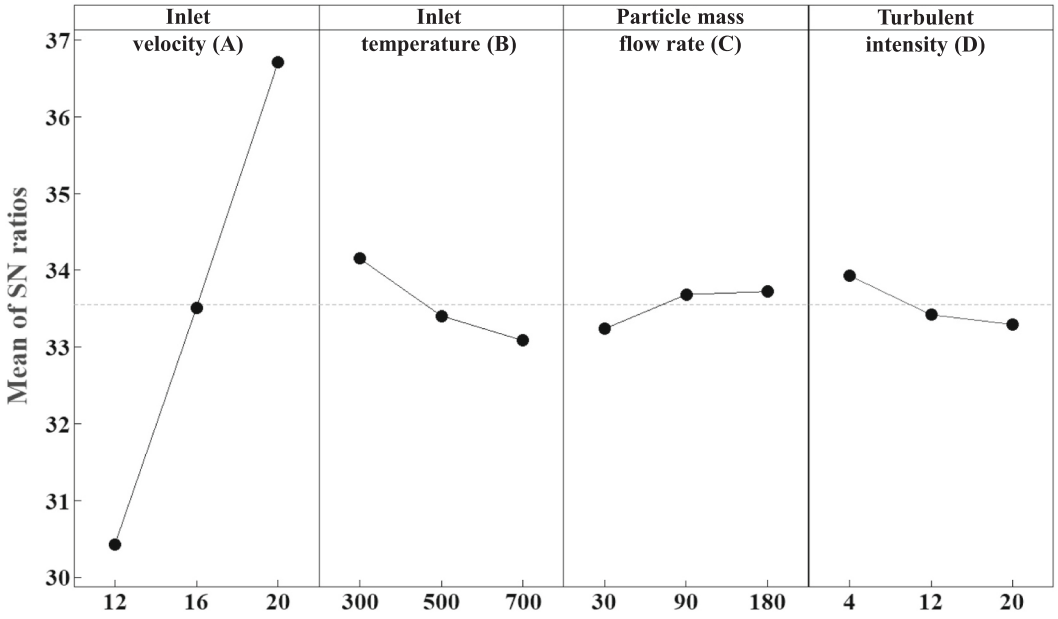

Fig. 6. The mean S/N ratio for parametric design.

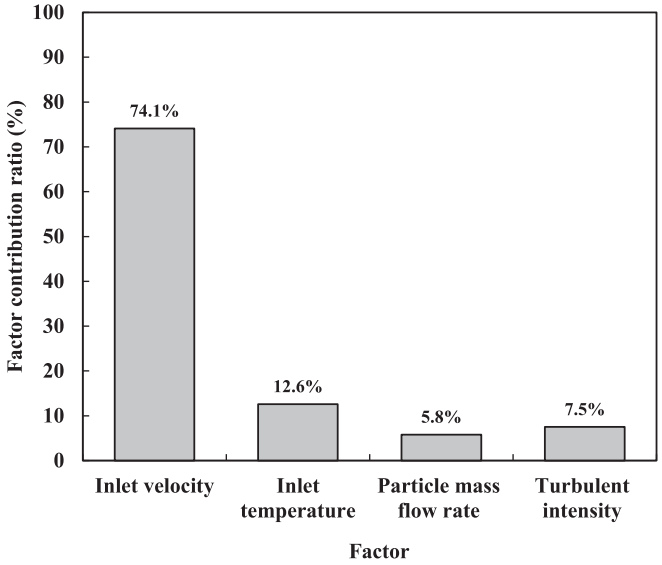

Fig. 7. Contribution ratio of A, B, C, and D (factors).

found that increasing the inlet temperature dropped tangential velocity considerably. The highest tangential velocity in the optimized square cyclone (E7) is determined to be around 17.5 m/s, while the peak tangential velocity in the E3 case is estimated to be 10.2 m/s. As a result, the optimized case produced a more intense centrifugal force field in the square cyclone than the E3 case, and hence an improved collection efficiency would be predicted.

Table 7
Regression analysis for response parameter versus factors.

Term	Coef	SE Coef	T-Value	P-Value
Constant	−14.02	6.37	−2.20	0.092
A	4.417	0.307	14.40	0.000
B	−0.01417	0.00613	−2.31	0.082
C	0.0275	0.0162	1.69	0.166
D	−0.210	0.153	−1.37	0.242

Table 8
Analysis of variance for regression.

Source	DF	Adj SS	Adj MS	F-Value	P-Value
Regression	4	1963.67	490.92	54.37	0.001
A	1	1872.67	1872.67	207.40	0.000
B	1	48.17	48.17	5.33	0.082
C	1	25.84	25.84	2.86	0.166
D	1	17.00	17.00	1.88	0.242
Error	4	36.12	9.03		
Total	8	1999.79			

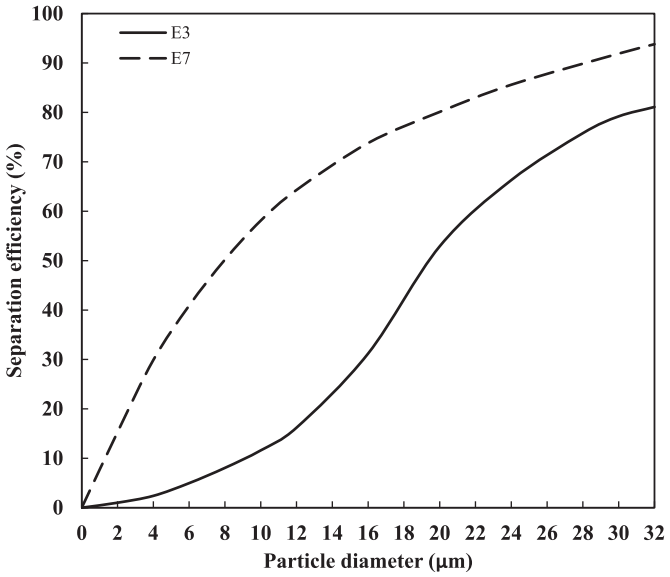

Fig. 8. Change of separation efficiency versus particle size for E3 and E7 cases.

3.9. Motion of particles

Fig. 10 shows the movements of particles inside a gas cyclone for a time period of 0.8 s for two cases (i.e., E3 and E7) which offer the lowest and maximum separation efficiency. This figure describes the dispersion of particle clouds with sizes (1 to 16 μm) which depicts the temporal evolution variances in configurations of motion of particles. In both situations, particles entered the square cyclone and traveled downward to the cyclone's main body, which behaved as the separation zone. Particles were separated from the gas by deposition on the wall surface due to centrifugal force and on the bottom surface due to gravity sedimentation. The recirculation gas flow caused larger particles for accumulating at the top of the main section, leading to a higher particle concentration in this region. As a result, certain particles in the gas were unable to be separated. Higher inlet velocity and particle mass loading levels in case E7 resulted in more particles accumulating at the conical bottom portion and quickly being trapped. While the chance of separation was lowered in case E3, where the centrifugal force was substantially reduced due to the inlet temperature of 700 K.

3.10. Confirmation test

Table 9 summarizes the confirmation test results, with both the predicted and observed separation efficiencies. The table demonstrates that the anticipated and observed values match quite well. The findings reveal that the improvement in the S/N ratio for separation efficiency is 0.59 dB. The separation efficiency was also improved by around 3.5%. Confirmation tests validated the reliability of the Taguchi method adopted in design parameter optimization.

4. Conclusions

A numerical methodology based on a three-dimensional CFD analysis and the Taguchi approach was proposed to assess the square cyclone performance and determine the optimum operating parameters that would result in the highest separation efficiency of the system. The Taguchi technique was implemented to observe the optimum working condition parameters and to evaluate the selected factors' impact on the square cyclone. An L_9 orthogonal array was applied to examine four operating condition factors (i.e., inlet temperature, inlet velocity, particle mass flow rate, and turbulent intensity), as well as three levels.

The reliability of the CFD modeling was confirmed by comparing the results with the experimental test of Su and Mao [28], as well as the numerical simulations conducted by Su et al. [50]. The comparison showed a good level of agreement. The ANOVA analysis revealed that inlet velocity was the most significant factor in influencing cyclone efficiency, followed by inlet temperature and particle mass flow rate. The optimal operating condition parameters were found to be $A_3B_1C_3$, which represents 20 m/s inlet velocity, inlet temperature (300 K), 180 g/min particle mass flow rate, and 4% turbulent intensity. The separation efficiency for a particle diameter of 16 μm achieved 76% with these optimized values.

CRediT authorship contribution statement

Hossein Fatahian: Writing – original draft, Conceptualization, Validation, Visualization, Methodology, Software. **Esmaeel Fatahian:** Investigation, Methodology, Formal analysis, Resources, Writing –

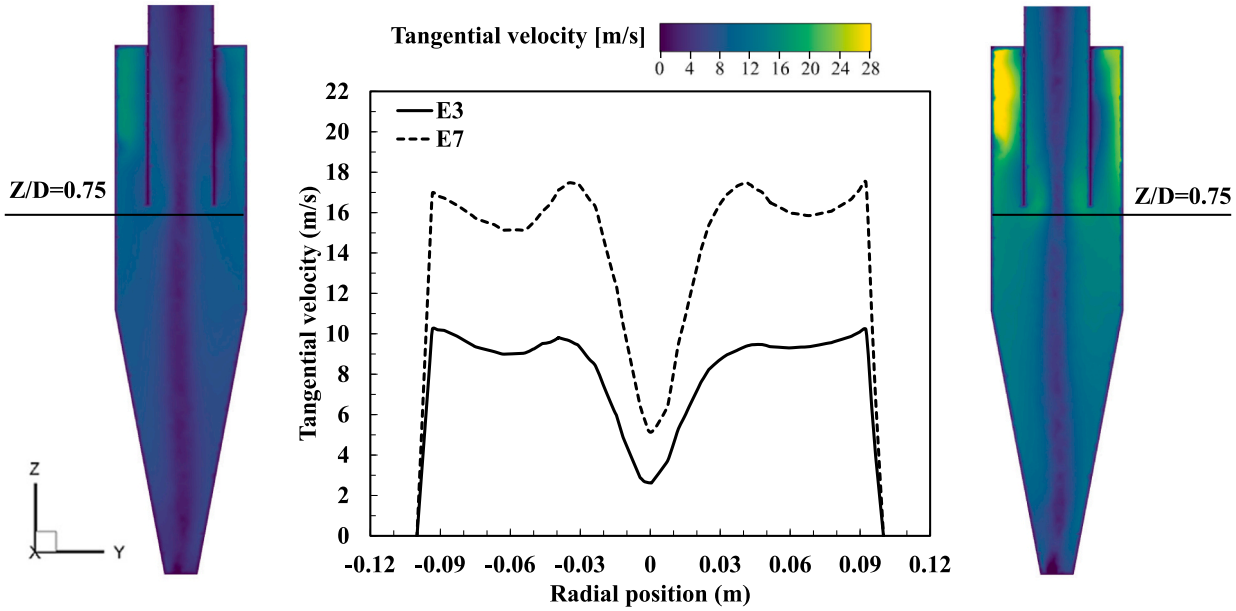

Fig. 9. Comparison of tangential velocity contours and profiles at position z/D = 0.75 for E3 and E7 cases.

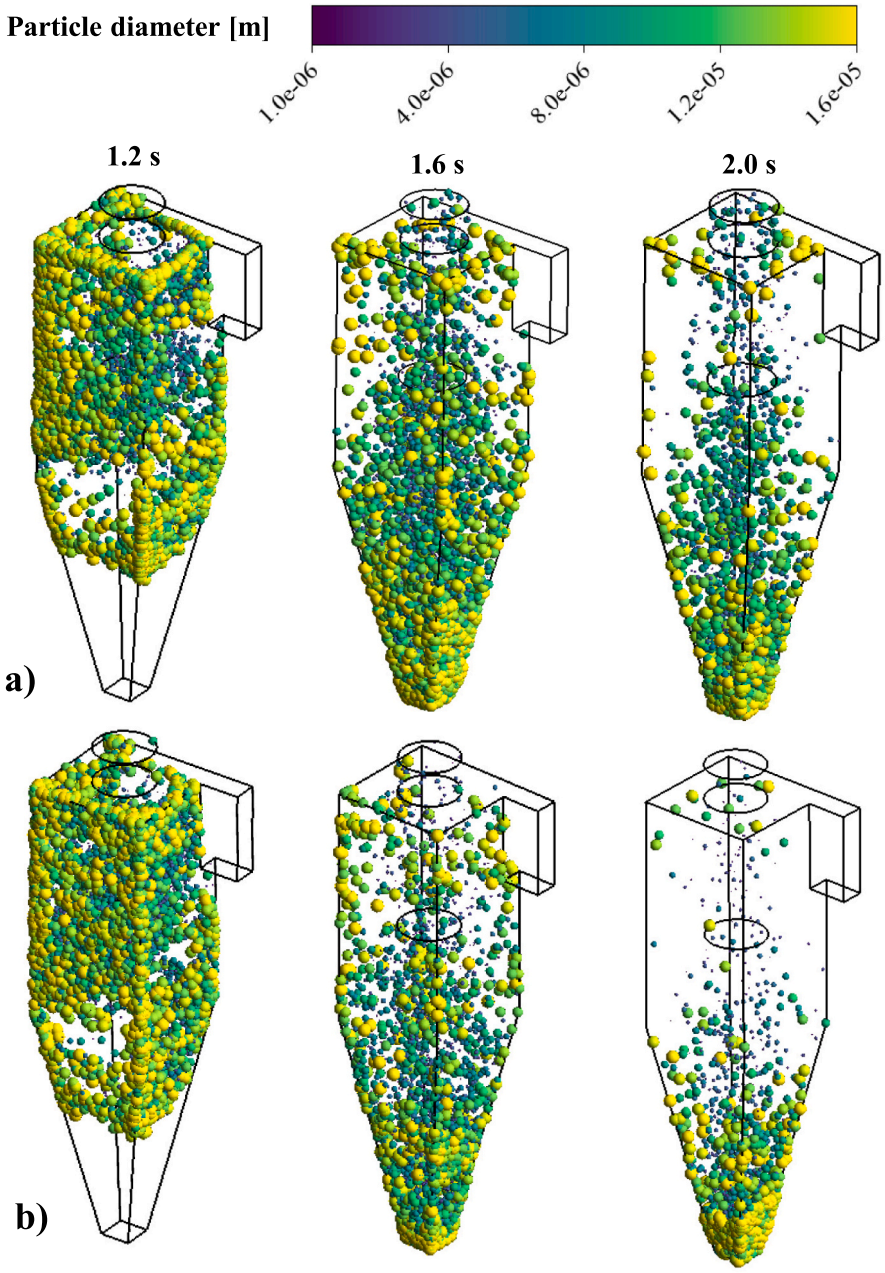

Fig. 10. Particles motion for a) E3 b) E7 cases.

Table 9
Comparing the predicted and observed values.

	Initial parameter	Optimum parameter	
		Predicted	Experiment
Levels	A3B1C3D2	A3B1C3D1	A3B1C3D1
Separation efficiency (%)	73.8	75.6	76.4
S/N ratio (dB)	37.36	37.87	37.95

review & editing. **Rasool Erfani:** Investigation, Writing – review & editing, Supervision.

Declaration of Competing Interest

The authors declare that they have no known competing financial interests or personal relationships that could have appeared to influence the work reported in this paper.

Data availability

Data will be made available on request.

References

[1] H. Yoshida, Effect of apex cone shape and local fluid flow control method on fine particle classification of gas-cyclone, Chem. Eng. Sci. 85 (2013) 55–61.

[2] K. Elsayed, F. Parvaz, S.H. Hosseini, G. Ahmadi, Influence of the dipleg and dustbin dimensions on performance of gas cyclones: an optimization study, Sep. Purif. Technol. 239 (2020), 116553.
[3] H. Yang, N. Wang, Y. Cao, X. Meng, L. Yao, Effects of helical fins on the performance of a cyclone separator: A numerical study, Adv. Powder Technol. 34 (1) (2023), 103929.
[4] E. Yohana, M. Tauviqirrahman, B. Yusuf, K.H. Choi, V. Paramita, Effect of vortex limiter position and metal rod insertion on the flow field, heat rate, and performance of cyclone separator, Powder Technol. 377 (2021) 464–475.
[5] E. Hosseini, H. Fatahian, E. Fatahian, New understanding of the effect of particle mass loading on the performance of a square cyclone at low and high gas temperatures, Korean J. Chem. Eng. 39 (12) (2022) 3482–3496.
[6] E. Fatahian, H. Fatahian, E. Hosseini, G. Ahmadi, A low-cost solution for the collection of fine particles in square cyclone: A numerical analysis, Powder Technol. 387 (2021) 454–465.
[7] Z. Wang, G. Sun, Z. Song, S. Yuan, Z. Qian, Effect of inlet volute wrap angle on the flow field and performance of double inlet gas cyclones, Particuology 77 (2023) 29–36.
[8] H. Fatahian, E. Fatahian, M.E. Nimvari, Improving efficiency of conventional and square cyclones using different configurations of the laminarizer, Powder Technol. 339 (2018) 232–243.
[9] M. Wasilewski, L.S. Brar, G. Ligus, Experimental and numerical investigation on the performance of square cyclones with different vortex finder configurations, Sep. Purif. Technol. 239 (2020), 116588.
[10] S. Venkatesh, R.S. Kumar, S.P. Sivapirakasam, M. Sakthivel, D. Venkatesh, S. Y. Arafath, Multi-objective optimization, experimental and CFD approach for performance analysis in square cyclone separator, Powder Technol. 371 (2020) 115–129.
[11] H. Safikhani, M. Shams, S. Dashti, Numerical simulation of square cyclones in small sizes, Adv. Powder Technol. 22 (3) (2011) 359–365.
[12] N. Malahayati, D. Darmadi, C.A. Putri, L. Mairiza, W. Rinaldi, Y. Yunardi, Comparative performance analysis between conventional and square cyclones for solid particle-gas separation: A review, Mater. Today: Proc. 63 (1) (2022) S318–S325.
[13] A.N. Huang, N. Maeda, D. Shibata, T. Fukasawa, H. Yoshida, H.P. Kuo, K. Fukui, Influence of a laminarizer at the inlet on the classification performance of a cyclone separator, Sep. Purif. Technol. 174 (2017) 408–416.
[14] I. Karagoz, A. Avci, A. Surmen, O. Sendogan, Design and performance evaluation of a new cyclone separator, J. Aerosol Sci. 59 (2013) 57–64.
[15] S. Venkatesh, S.P. Sivapirakasam, M. Sakthivel, S. Ganeshkumar, M.M. Prabhu, M. Naveenkumar, Experimental and numerical investigation in the series arrangement square cyclone separator, Powder Technol. 383 (2021) 93–103.
[16] H. Fatahian, E. Fatahian, M.E. Nimvari, G. Ahmadi, Novel designs for square cyclone using rounded corner and double-inverted cones shapes, Powder Technol. 380 (2021) 67–79.
[17] H. Fatahian, E. Hosseini, E. Fatahian, CFD simulation of a novel design of square cyclone with dual-inverse cone, Adv. Powder Technol. 31 (4) (2020) 1748–1758.
[18] H. Safikhani, M. Rafiee, D. Ashtiani, Numerical study of flow field in new design cyclones with different wall temperature profiles: comparison with conventional ones, Adv. Powder Technol. 32 (9) (2021) 3268–3277.
[19] E. Hosseini, H. Fatahian, G. Ahmadi, M. Eshagh Nimvari, E. Fatahian, CFD study on the effect of gas temperature on the separation efficiency of square cyclones, J. Braz. Soc. Mech. Sci. Eng. 43 (9) (2021) 1–13.
[20] M. Siadaty, S. Kheradmand, F. Ghadiri, Research on the effects of operating conditions and inlet channel configuration on exergy loss, heat transfer and irreversibility of the fluid flow in single and double inlet cyclones, Appl. Therm. Eng. 137 (2018) 329–340.
[21] J. Gimbun, T.G. Chuah, Fakhru'l-Razi, A., & Choong, T. S., The influence of temperature and inlet velocity on cyclone pressure drop: a CFD study, Chem. Eng. Process. Process Intensif. 44 (1) (2005) 7–12.
[22] M. Siadaty, S. Kheradmand, F. Ghadiri, Study of inlet temperature effect on single and double inlets cyclone performance, Adv. Powder Technol. 28 (6) (2017) 1459–1473.
[23] F. Qian, Z. Huang, G. Chen, M. Zhang, Numerical study of the separation characteristics in a cyclone of different inlet particle concentrations, Comput. Chem. Eng. 31 (9) (2007) 1111–1122.
[24] P. Kozołub, A. Klimanek, R.A. Białecki, W.P. Adamczyk, Numerical simulation of a dense solid particle flow inside a cyclone separator using the hybrid Euler–Lagrange approach, Particuology 31 (2017) 170–180.
[25] S.G. Bogodage, A.Y.T. Leung, Improvements of the cyclone separator performance by down-comer tubes, J. Hazard. Mater. 311 (2016) 100–114.
[26] A.N. Huang, K. Ito, T. Fukasawa, K. Fukui, H.P. Kuo, Effects of particle mass loading on the hydrodynamics and separation efficiency of a cyclone separator, J. Taiwan Inst. Chem. Eng. 90 (2018) 61–67.
[27] G. Wan, G. Sun, X. Xue, M. Shi, Solids concentration simulation of different size particles in a cyclone separator, Powder Technol. 183 (1) (2008) 94–104.
[28] Y. Su, Y. Mao, Experimental study on the gas–solid suspension flow in a square cyclone separator, Chem. Eng. J. 121 (1) (2006) 51–58.
[29] W.D. Griffiths, F. Boysan, Computational fluid dynamics (CFD) and empirical modelling of the performance of a number of cyclone samplers, J. Aerosol Sci. 27 (2) (1996) 281–304.
[30] K. Elsayed, C. Lacor, Modeling and Pareto optimization of gas cyclone separator performance using RBF type artificial neural networks and genetic algorithms, Powder Technol. 217 (2012) 84–99.
[31] E. Hosseini, M.A. Atarzadeh, M. Shekarzadeh, Effect of erosion rate and particle mass loading on separation efficiency of square cyclone by considering gas temperature, Journal of the Brazilian Society of Mechanical Sciences and Engineering 44 (9) (2022) 411.
[32] H. Fatahian, E. Fatahian, Improving the efficiency of a square cyclone separator using the Dipleg–A CFD-based analysis, Iran. J. Chem. Chem. Eng. 41 (2) (2022) 670–681.
[33] E. Hosseini, Performance assessment of a square cyclone influenced by inlet section modifications, J. Braz. Soc. Mech. Sci. Eng. 42 (10) (2020) 1–11.
[34] O.R. Nassaj, D. Toghraie, M. Afrand, Effects of multi-inlet guide channels on the performance of a cyclone separator, Powder Technol. 356 (2019) 353–372.
[35] K. Jang, G.G. Lee, K.Y. Huh, Evaluation of the turbulence models for gas flow and particle transport in URANS and LES of a cyclone separator, Comput. Fluids 172 (2018) 274–283.
[36] L. Qiang, W. Qinggong, X. Weiwei, Z. Zilin, Z. Konghao, Experimental and computational analysis of a cyclone separator with a novel vortex finder, Powder Technol. 360 (2020) 398–410.
[37] B.E. Launder, G.J. Reece, W. Rodi, Progress in the development of a Reynolds-stress turbulence closure, J. Fluid Mech. 68 (3) (1975) 537–566.
[38] G. Wan, G. Sun, X. Xue, M. Shi, Solids concentration simulation of different size particles in a cyclone separator, Powder Technol. 183 (1) (2008) 94–104.
[39] A.J. Hoekstra, J.J. Derksen, H.E.A. Van Den Akker, An experimental and numerical study of turbulent swirling flow in gas cyclones, Chem. Eng. Sci. 54 (13–14) (1999) 2055–2065.
[40] K. Elsayed, C. Lacor, Optimization of the cyclone separator geometry for minimum pressure drop using mathematical models and CFD simulations, Chem. Eng. Sci. 65 (22) (2010) 6048–6058.
[41] K. Elsayed, C. Lacor, The effect of the dust outlet geometry on the performance and hydrodynamics of gas cyclones, Comput. Fluids 68 (2012) 134–147.
[42] S.A.J. Morsi, A.J. Alexander, An investigation of particle trajectories in two-phase flow systems, J. Fluid Mech. 55 (2) (1972) 193–208.
[43] K. Elsayed, C. Lacor, Numerical modeling of the flow field and performance in cyclones of different cone-tip diameters, Comput. Fluids 51 (1) (2011) 48–59.
[44] F. Parvaz, S.H. Hosseini, K. Elsayed, G. Ahmadi, Numerical investigation of effects of inner cone on flow field, performance and erosion rate of cyclone separators, Sep. Purif. Technol. 201 (2018) 223–237.
[45] C. Song, B. Pei, M. Jiang, B. Wang, D. Xu, Y. Chen, Numerical analysis of forces exerted on particles in cyclone separators, Powder Technol. 294 (2016) 437–448.
[46] K. Elsayed, C. Lacor, Modeling and Pareto optimization of gas cyclone separator performance using RBF type artificial neural networks and genetic algorithms, Powder Technol. 217 (2012) 84–99.
[47] M. Wasilewski, L.S. Brar, Effect of the inlet duct angle on the performance of cyclone separators, Sep. Purif. Technol. 213 (2019) 19–33.
[48] M.S. Shin, H.S. Kim, D.S. Jang, J.D. Chung, M. Bohnet, A numerical and experimental study on a high efficiency cyclone dust separator for high temperature and pressurized environments, Appl. Therm. Eng. 25 (11−12) (2005) 1821–1835.
[49] A. Jafarnezhad, H. Salarian, S. Kheradmand, J. Khaleghinia, Performance improvement of a cyclone separator using different shapes of vortex finder under high-temperature operating condition, J. Braz. Soc. Mech. Sci. Eng. 43 (2) (2021) 1–15.
[50] Y. Su, A. Zheng, B. Zhao, Numerical simulation of effect of inlet configuration on square cyclone separator performance, Powder Technol. 210 (3) (2011) 293–303.
[51] R. Erfani, T. Erfani, C. Hale, K. Kontis, S. Utyuzhnikov, Optimization of induced velocity for plasma actuator with multiple encapsulated electrodes using response surface methodology, in: 49th AIAA Aerospace Sciences Meeting including the New Horizons Forum and Aerospace Exposition, 2011, January, p. 1206.
[52] X. Sun, S. Kim, S.D. Yang, H.S. Kim, J.Y. Yoon, Multi-objective optimization of a Stairmand cyclone separator using response surface methodology and computational fluid dynamics, Powder Technol. 320 (2017) 51–65.
[53] T. Erfani, R. Erfani, Fair resource allocation using multi-population evolutionary algorithm", Applications of Evolutionary Computation, Lecture Notes in Computer Science (2015) 9028, https://doi.org/10.1007/978-3-319-16549-3_18.
[54] T. Erfani, R. Erfani, An evolutionary approach to solve a system of multiple interrelated agent problems, Applied Soft Computing 37 (2015) 40–47, https://doi.org/10.1016/j.asoc.2015.07.049.